

Explorations in Astrophysics

Tully Fisher for Disk Galaxies and Linearity of Dark Matter in Galaxy Clusters

Author:

Varenya UPADHYAYA
EP20BTECH11026

Supervisor:

Dr. Shantanu DESAI

November 26, 2022



Contents

0.1	Acknowledgements	2
1	The Tully-Fisher Relation	3
1.1	Abstract	3
1.2	Introduction	3
1.2.1	The Tully-Fisher Relation	3
1.2.2	Markov-Chain Monte Carlo Simulations: <code>emcee</code>	4
1.3	Data	5
1.3.1	Redshift $z \sim 0$	5
1.3.2	Redshift $z \sim 1$	5
1.4	Analysis and Results	6
1.4.1	$z \sim 0$	7
1.4.2	$z \sim 1$	8
1.5	Conclusions	14
2	Linearity and Universality of Dark Matter in Galaxy Clusters	15
2.1	Abstract	15
2.2	Introduction	15
2.3	Data and Analysis	16
2.4	Results	17
2.5	Conclusion	19

0.1 Acknowledgements

I am extremely grateful to Prof. Shantanu Desai for guiding me through this work and helping me out wherever I got stuck. I'm also grateful to Dr. Gauri Sharma for providing the data and the resources that made this work possible

Chapter 1

The Tully-Fisher Relation

1.1 Abstract

We study the Baryonic and Stellar Tully Fisher Relations at $z \sim 0$ using the SPARC sample which contains 153 galaxies to recreate the results in [Lel+19]. We then conduct a similar analysis on data of galaxies farther back in time $z \sim 1$ by investigating a sub-sample of the KMOS Redshift One Spectroscopic Survey (KROSS) as studied in [Sha+21]. We study 250 galaxies at $z \approx 0.9$ having a stellar mass range $9.0 < \log(M_* M_\odot) < 11.0$ whose circular velocities are obtained directly from the rotation curves at $2.95 R_e$. We find that our results for low redshifts are in agreement with the conclusions in [Lel+19]. For galaxies at $z \sim 1$, we find little to no correlation between the masses and velocities (ie. almost flat curves).

1.2 Introduction

1.2.1 The Tully-Fisher Relation

In 1977, two astronomers Brent Tully and Richard Fisher[TF77] discovered a surprisingly tight correlation between the luminosity and the HI line width of the global profiles of spiral galaxies. Luminosity and line width serve as proxies for the Mass and Asymptotic rotation velocities for the galaxies respectively. The relation has been extensively used as a distance indicator and although it has been studied for decades since its first release in 1977, the physical basis behind it is still unexplained.[FM12a]

The correlation improves as more accurate indicators of the quantities (mass, velocity) are used. For example, rotation curves where the flat parts of the curve (V_f) can be measured give tighter relations than those that only use the line-widths [Cou97]. Similarly near-infrared luminosities give lower scatter compared to optical luminosities as the former give more reliable mapping of starlight to star masses. [Bel+03]

A more fundamental relation occurs when total baryonic mass and the rotation velocity are considered. Since in most galaxies the stars constitute most of the baryonic mass, luminosity suffices as a good proxy for mass. However the interstellar media also consists of a considerable amount of baryons and this contribution is accounted for by calculating the mass of the neutral atomic hydrogen (HI). While the Luminous Tully-Fisher relation breaks down, but using the baryonic mass $M_{bar} = M_{star} + M_{gas}$ presents a relation that persists [McG+00]. This relation is referred to as the Baryonic Tully-Fisher relation.

The relation is given as a power law:

$$M_{bar} = \beta(V_f)^\alpha \quad (1.1)$$

or correspondingly,

$$\log M_{bar} = m \log V_f + b \quad (1.2)$$

When stellar mass is considered instead of the total mass, the relation is referred to as the Stellar Tully-Fisher relation.

$$\log M_{star} = m \log V_f + b \quad (1.3)$$

The physics behind the relation is still disputed. Λ CDM suggests a V_f^3 dependence with the total (baryonic+dark) mass rather than an explicit M_b v. V_f relation [SN99]. [KSW00] discusses the origin of the relation using an N-body simulation with for 14 galaxies and different masses/spin parameters in the Cold Dark Matter cosmology. The relation is consistent with a constant acceleration scale $a = V_f^4/GM_b$ such that the normalization constant $\beta = Ga$ [McG+00]

Nevertheless, the relation is often used to estimate distances and to constrain properties of dark matter and its relation with the visible matter [Tra+09]. Our work revolves around computing this relation using Eqs. (1.2), (1.3) for galaxies up to $z \sim 1$ and seeing its validity on our datasets.

1.2.2 Markov-Chain Monte Carlo Simulations: emcee

MCMC methods are generally used to numerically perform multidimensional integrals, and more often for fitting models to data [HF18]. They are used to sample data from a posterior distribution around certain optimum values to model the presented data. In essence, the whole process of using an MCMC simulation is to compare a model (generated using parameters) against the data and sample the parameters that best fit the data. These methods are inherently Bayesian (as they involve a prior range on the parameters) rather than frequentist.

The probability of a model given a data is (using Bayes theorem):

$$P(\theta|D) = \frac{P(D|\theta) \times P(\theta)}{P(D)} \quad (1.4)$$

where θ and D represent the Model and Data respectively. The terms in (1.4) are:

- $P(\theta|D)$: Posterior Probability (probability of the model given the data)
- $P(D|\theta)$: Likelihood (probability of the data given the model)
- $P(\theta)$: Prior (the probability of the model)
- $P(D)$: Evidence (probability of the data, usually taken as unity)

Using MCMC, we can estimate the posterior distribution by numerically integrating the RHS of (1.4). For the expectation value of θ , we would need:

$$E(\theta) = \int \theta p(\theta) d\theta \quad (1.5)$$

Numerically, this can be sampled as:

$$E(\theta) \approx \frac{1}{N} \sum_{n=1}^N \theta_n \quad (1.6)$$

In order to successfully run an MCMC, we employ the following steps:

1. Establish a function that outputs the model (in our case, a straight line)
2. Initialize an ensemble of "walkers" defined by θ , a vector of parameters that contains the parameters in question. For example, a simple linear fit will have a θ like:

$$\theta = \begin{pmatrix} m \\ b \end{pmatrix}, \quad (1.7)$$

with m and b as the slope and intercept respectively

3. Every walker now begins to explore the parameter space (bounded by the prior) by taking "steps" (or walking) to new values of θ . At each new value, a model is generated and it is then compared to the data using the likelihood function mentioned above. For a simple χ^2 likelihood (assuming a linear fit) this would look like:

$$-2\mathcal{L} = \sum \left(\frac{y_i - (mx_i + b)}{\sigma_y} \right)^2, \quad (1.8)$$

with σ_y representing the error in data.

4. MCMC then checks the ratio of \mathcal{L} generated by the new model v. the current model and moves to the new θ if it provides a better match. Often though, the MCMC doesn't move to the better θ and this is decided by something called the *acceptance ratio*. This ensures that the walkers don't get trapped on individual peaks of high probabilities.
5. Eventually the walkers all begin "climbing" to the models with high \mathcal{L} values.

After the code is done running (ie. the production run ends) we're left with a *posterior distribution* with every walker keeping a record of every θ it "walked" to. After running for long enough (assuming the MCMC converges) the distribution basically represents a sample of reasonable models for the data.

In our analysis, we make use of `emcee`[[For+13](#)], a python module which runs the MCMC simulations.

1.3 Data

We conducted our analysis on two sets of data – one on nearby galaxies (zero redshift) and another on galaxies farther out (one redshift)

1.3.1 Redshift $z \sim 0$

For $z \sim 0$ we use the SPARC (Spitzer Photometry & Accurate Rotation Curves) database [[LMS16](#)] which is a sample of 175 nearby galaxies. The database contains the HI rotation curves accumulated over 3 decades of radio interferometry and homogeneous near-IR photometry. The data can be found at [SPARC Homepage](#). For our analysis, we use the `table` provided under the Baryonic Tully Fisher Relation section. The data contains the baryonic masses and velocities for the galaxies. There are multiple velocity definitions used in the data:

Velocity Definitions

1. W_{P20} is the line-width measured at 20% of the peak flux density of the global H I profile (as used in [[TF77](#)]). Half of this width corresponds to the circular velocity in the outer parts of the H I disc
2. W_{M50} is the line-width measured at 50% of the mean flux density of the global H I profile. $W_{M50} < W_{P20}$ [[Cou+09](#)], implying that W_{M50} probes velocities at smaller radii.
3. V_{\max} is the circular velocity measured at the peak of the observed rotation curve. Since galaxy discs can show significant deviations from exponential profiles, usually $V_{\max} < V_{2.2}$
4. V_{2R_e} is the circular velocity measured at $2R_e$ where R_e is the effective radius encompassing half of the galaxy luminosity.
5. $V_{2.2}$ is the circular velocity measured at $2.2R_d$ (R_d is the disc scale length)
6. V_f is the average circular velocity along the flat part of the rotation curve.

Since both V_f and V_{\max} are dealing with the flat parts of the rotation curves, they depend on the shapes of the curves. For galaxies with rising rotation curves, these definitions become ambiguous. A more detailed discussion of the velocities can be found in [[Lel+19](#)]

1.3.2 Redshift $z \sim 1$

For higher redshifts, we used the KROSS data [[Sto+16](#)]. The KMOS Redshift One Spectroscopic Survey (KROSS) is an ESO-guaranteed time survey of 795 typical star-forming galaxies in the redshift range $z = 0.8\text{--}1.0$ with the KMOS instrument on the Very Large Telescope. Out of these, [[Sha+21](#)] analysed 344 galaxies out of which we use 250 galaxies for our purposes. The analysed data investigated the circular velocity at three length scales:

1. R_e (Effective radius)
2. $R_{opt} = 3.2R_D$ (Optical radius)

3. $R_{out} = 6.4R_D$ (Twice the optical radius)

where, $R_D=0.59R_e$ is the disk length

Since the effective radius for the majority of samples falls below resolution limit and the optical radius stays on the verge[Sha+21], our analysis is restricted to the measurements done at R_{out} . All in all, we use the velocity definitions at R_{out} to compute the Baryonic and Stellar Tully-Fisher Relations at $z \sim 1$

1.4 Analysis and Results

1. add the cornerplots and bestfit curves for both $z=0,1$
2. explain the cornerplots and bestfit

The TFR for Baryonic and Stellar masses is given as:

$$\log(M_{bar}) = m \log(V_f) + b \quad (1.9)$$

$$\log(M_{star}) = m \log(V_f) + b \quad (1.10)$$

We make use of `emcee` to sample the likelihood with the following priors:

- uniform prior for both intercept and slope $m, b \in [-10, 10]$
- uniform prior for the intrinsic scatter $\sigma_{int} \in [-1, 1]$

For our analysis, we employed three key likelihood functions:

1. A χ^2 likelihood (as discussed in 1.2.2 that follows:

$$-2\mathcal{L} = \sum \left(\frac{y_i - (mx_i + b)}{\sigma_y} \right)^2, \quad (1.11)$$

2. A simple log-likelihood (\mathcal{L}_1 from here on) that incorporates both errors in x and y: (chiefly used in [Lel+19])

$$-2\ln\mathcal{L}_1 = \sum_i (2\pi\sigma_i^2) + \sum_i \frac{(y_i - mx_i - c)^2}{\sigma_i^2} \quad (1.12)$$

$$\sigma_i^2 = m^2\sigma_{x_i}^2 + \sigma_{y_i}^2 + \sigma_{int}^2 \quad (1.13)$$

where σ_i represents the intrinsic scatter (a measure of how much the model deviates from the data).

3. A slightly more complicated routine (\mathcal{L}_2 from here on) that involves an extra slope term in the denominator (as used in Eq. 4-5 of[Tia+20])

$$-2\ln\mathcal{L}_2 = \sum_i (2\pi\sigma_i^2) + \sum_i \frac{(y_i - mx_i - c)^2}{\sigma_i^2(m^2 + 1)} \quad (1.14)$$

$$\sigma_i^2 = \frac{m^2\sigma_{x_i}^2 + \sigma_{y_i}^2}{m^2 + 1} + \sigma_{int}^2 \quad (1.15)$$

In the above equations $\{y_i, x_i\}$ represent the data for $\{\log(M), \log(v)\}$ (where M can be either baryonic or stellar mass) with $\{\sigma_y, \sigma_x\}$ denoting the errors in both the values respectively.

For all 3 likelihoods, we ran tests on the two datasets using 100 walkers and 3000 ensemble points for the walkers. For each walker, we initialize three values (for the slope, intercept and intrinsic scatter) drawn randomly from a uniform distribution for the prior range and use this as the initial state of the each of the walkers respectively. After successfully running the ensembler, we're left with the best fit parameters. The results for the data are as follows:

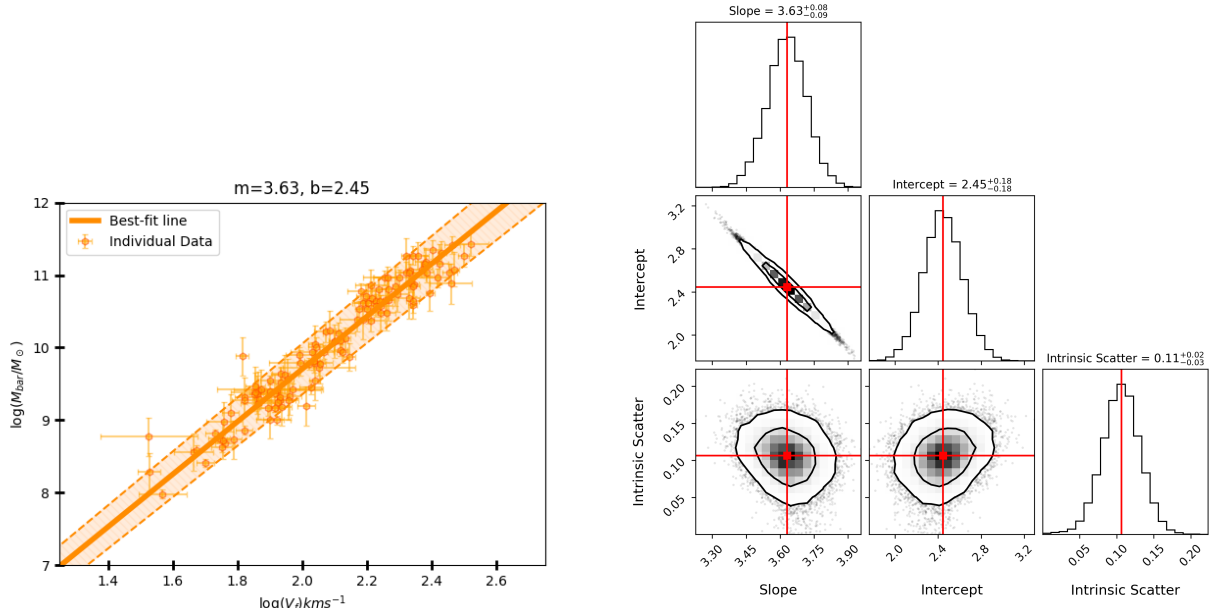
1.4.1 $z \sim 0$

Table 1.1 shows the results we got for the different velocity definitions using the \mathcal{L}_1 likelihood and find that these results are in agreement with the results in [Lel+19]. This serves as a code check, which will come in handy in the next part. It is easy to see that the steepest slope and lowest scatter happens for V_f

Velocity	Slope	Intercept	Intrinsic Scatter	Number of galaxies
V_f	$3.63^{+0.08}_{-0.09}$	$2.45^{+0.18}_{-0.18}$	$0.11^{+0.02}_{-0.03}$	123
$W_{P20/2}$	$3.53^{+0.07}_{-0.07}$	$1.37^{+0.18}_{-0.18}$	$0.13^{+0.02}_{-0.02}$	148
$W_{M50/2}$	$3.40^{+0.09}_{-0.09}$	$1.79^{+0.21}_{-0.21}$	$0.13^{+0.02}_{-0.02}$	125
V_{\max}	$3.31^{+0.07}_{-0.07}$	$3.04^{+0.15}_{-0.15}$	$0.15^{+0.02}_{-0.02}$	153
V_{2R_e}	$2.92^{+0.07}_{-0.07}$	$4.00^{+0.15}_{-0.15}$	$0.17^{+0.02}_{-0.02}$	142
$V_{2.2}$	$2.81^{+0.07}_{-0.07}$	$4.27^{+0.15}_{-0.15}$	$0.21^{+0.02}_{-0.02}$	148

Table 1.1: The best fit parameters for different velocity definitions in the SPARC data using \mathcal{L}_1

We show the best-fit and corner plots for V_f (the velocity definition that found the lowest intrinsic scatter) in Fig. 1.1



(a) A plot of the data points (along with the errorbars) over the model. The shaded region accounts for the errors tributions for the parameters. The red lines intersect at in the m and b values.
(b) The cornerplot for V_f which depicts the posterior distributions for the parameters. The red lines intersect at the maximum likelihood values. The two black contours in each plot represent the 1σ and 2σ confidence levels

Figure 1.1: The best fit and corner plot for V_f using our likelihood.

Fig. 1.2 shows the best-fit plots for all the different velocity definitions

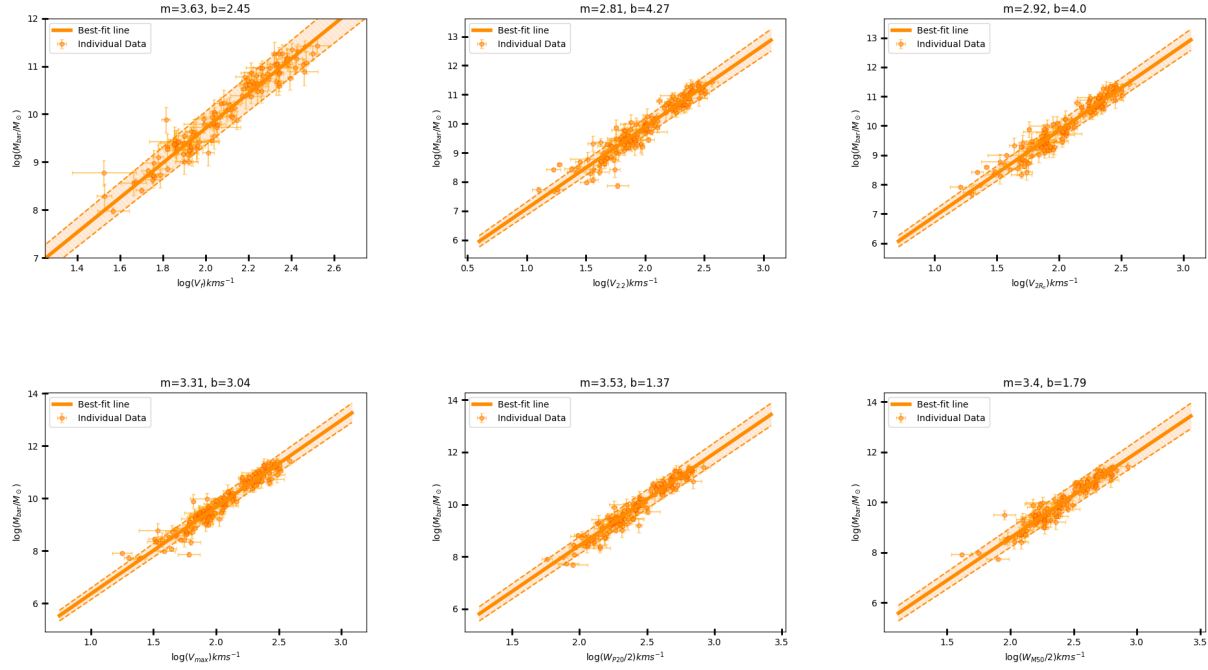


Figure 1.2: The BTFR for different velocity definitions: V_f (top left), $V_{2,2}$ (top middle), V_{2R_e} (top right), V_{\max} (bottom left), $W_{P20}/2$ (bottom middle), and $W_{M50}/2$ (bottom right). The black line shows a linear fit to the data. The tightest and steepest BTFR is given by V_f

1.4.2 $z \sim 1$

For galaxies in the one redshift range, we first ran our code for masses that were calculated using certain scaling relations that are powerful enough to give the total masses of the systems. Since circular velocities are only computed up to the visible domain, we later scaled these masses down using a Sersic Profile [Ser63]:

$$M_{gas}(R) = M_{gas} \left\{ 1 - \left(1 + \frac{R}{R_D} \right) e^{-R/R_D} \right\} \quad (1.16)$$

$$M_{star}(R) = M_{star} \left\{ 1 - \left(1 + \frac{R}{R_D} \right) e^{-R/R_D} \right\} \quad (1.17)$$

where, $R = R_{out}$, $R_D = 0.59R_e$. Table 1.2 contains the bestfit parameters for the three likelihoods discussed before, for the total masses. As seen from the slopes, the analysis points to anticorrelation (or none at all) between the masses and velocities.

Likelihood	Mass	m	b	σ_{int}
χ^2	Baryonic	$-0.09^{+0.14}_{-0.14}$	$11.28^{+0.30}_{-0.31}$	—
χ^2	Stellar	$+0.86^{+0.07}_{-0.07}$	$8.14^{+0.16}_{-0.16}$	—
\mathcal{L}_1	Baryonic	$-0.09^{+0.14}_{-0.14}$	$11.26^{+0.30}_{-0.30}$	$0.00^{+0.06}_{-0.06}$
\mathcal{L}_1	Stellar	$+0.91^{+0.13}_{-0.13}$	$8.04^{+0.28}_{-0.29}$	$0.26^{+0.02}_{-0.02}$
\mathcal{L}_2	Baryonic	$-0.02^{+0.03}_{-0.03}$	$10.96^{+0.70}_{-0.70}$	$0.14^{+0.01}_{-0.01}$
\mathcal{L}_2	Stellar	$+3.95^{+0.73}_{-0.57}$	$1.38^{+1.26}_{-1.59}$	$0.00^{+0.02}_{-0.02}$

Table 1.2: The best fit parameters for the KROSS data before scaling the masses

Fig 1.3 contains the best-fit and posterior distribution for the BTFR data in Table 1.2

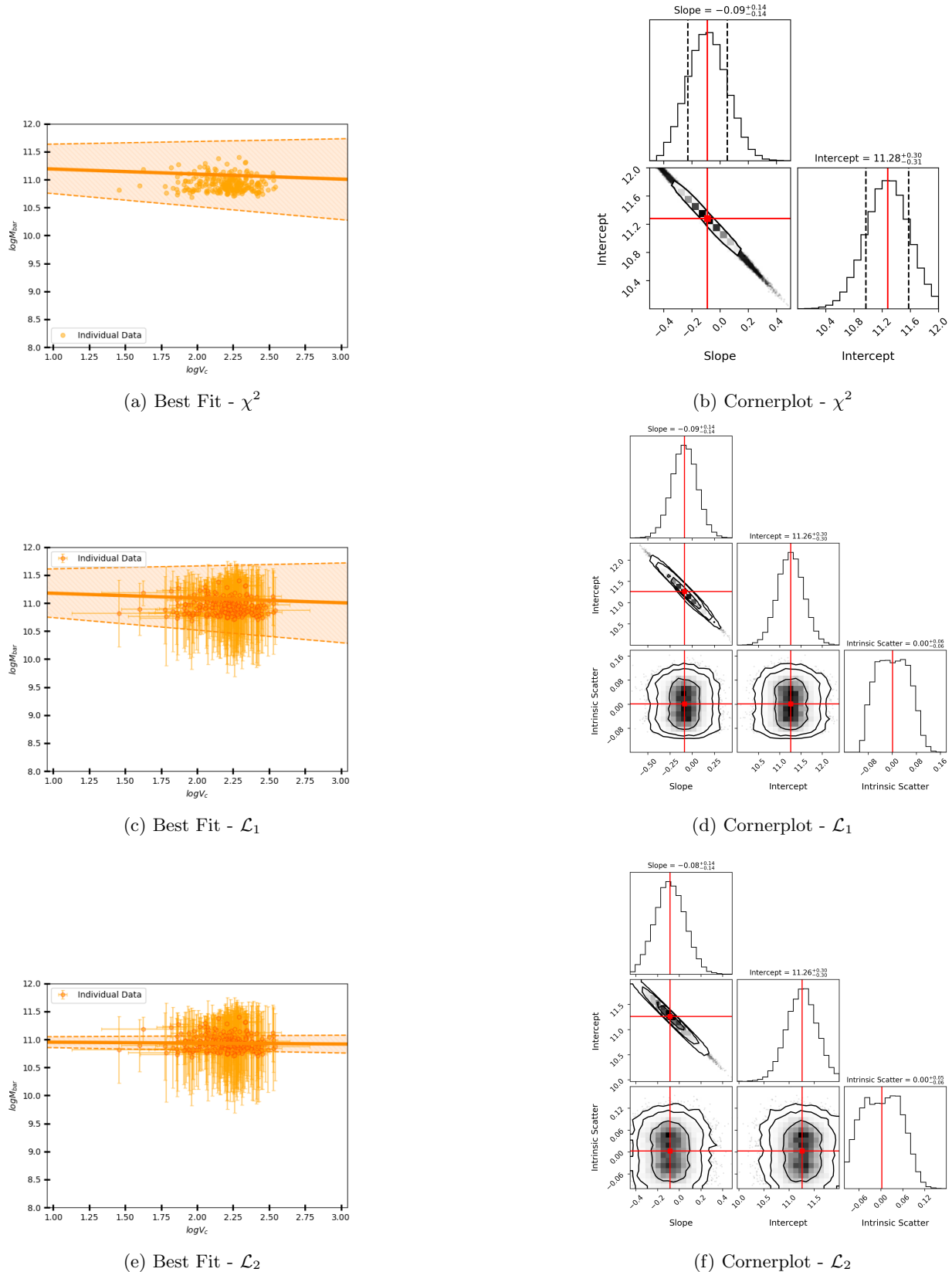


Figure 1.3: BTFR– The posterior distribution and best-fit plots for the full masses using the three likelihoods.

We scale the masses down using Eq 1.16, 1.17 with the appropriate values for R, R_D and redo our analysis

to attain the values in Table 1.3.

Likelihood	Mass	m	b	σ_{int}
χ^2	Baryonic	$0.16^{+0.11}_{-0.11}$	$10.18^{+0.24}_{-0.24}$	8.16
χ^2	Stellar	$0.90^{+0.08}_{-0.08}$	$8.02^{+0.18}_{-0.18}$	29.94
\mathcal{L}_1	Baryonic	$0.17^{+0.13}_{-0.12}$	$10.13^{+0.28}_{-0.28}$	$0.09^{+0.02}_{-0.03}$
\mathcal{L}_1	Stellar	$1.03^{+0.15}_{-0.15}$	$7.75^{+0.32}_{-0.33}$	$0.26^{+0.02}_{-0.02}$
\mathcal{L}_2	Baryonic	$0.80^{+0.16}_{-0.14}$	$8.70^{+0.30}_{-0.35}$	$0.11^{+0.03}_{-0.03}$
\mathcal{L}_2	Stellar	$4.02^{+0.74}_{-0.62}$	$1.11^{+1.36}_{-1.59}$	$0.00^{+0.02}_{-0.02}$

Table 1.3: The best fit parameters for the KROSS data after scaling the masses

The corresponding plots for these can be seen in Fig. 1.4

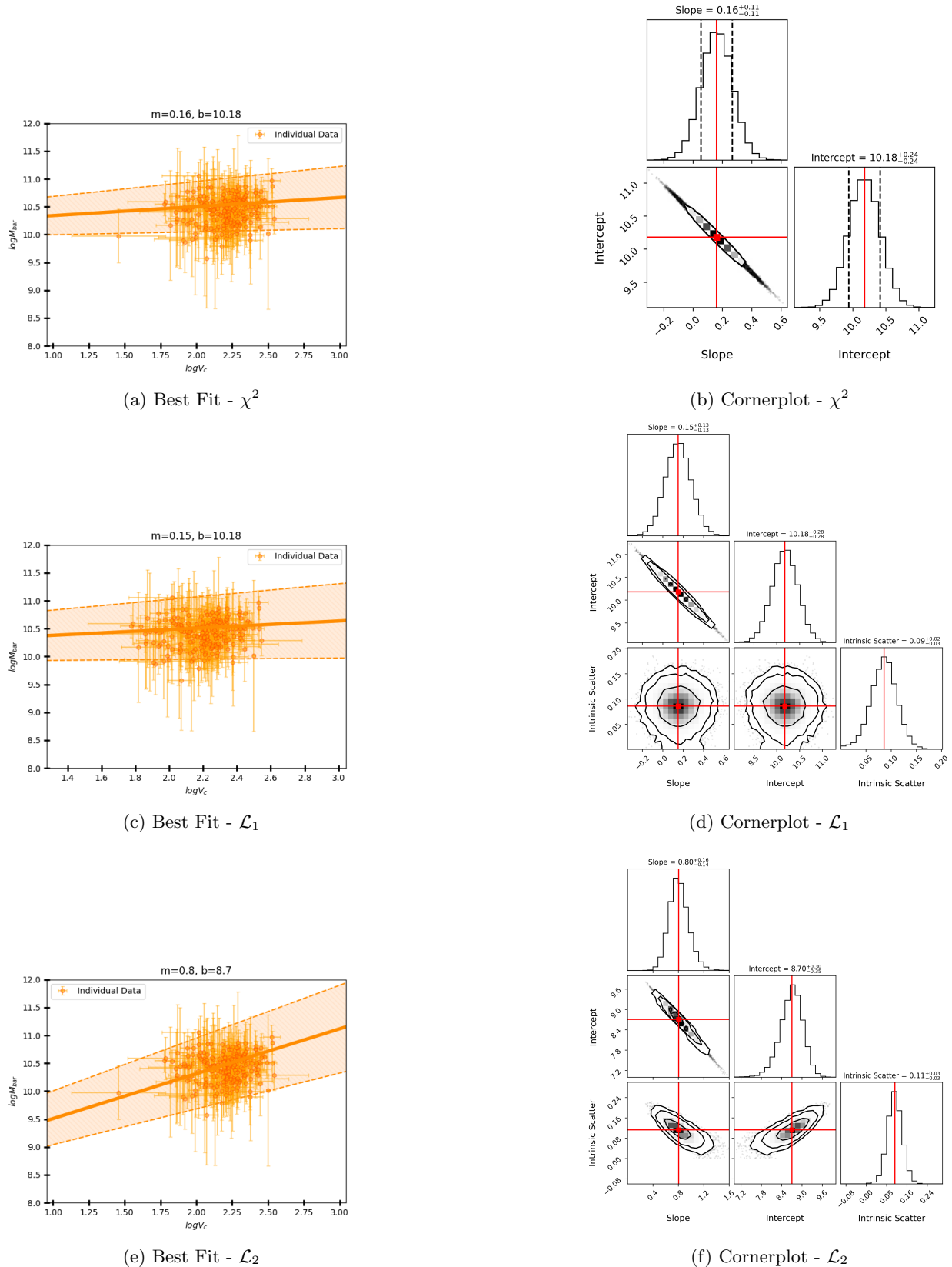


Figure 1.4: BTFR– The posterior distribution and best-fit plots for the sersic masses using the three likelihoods.

The figures for the STFR's using both the mass definitions can also be seen in Figs. 1.5 and 1.6

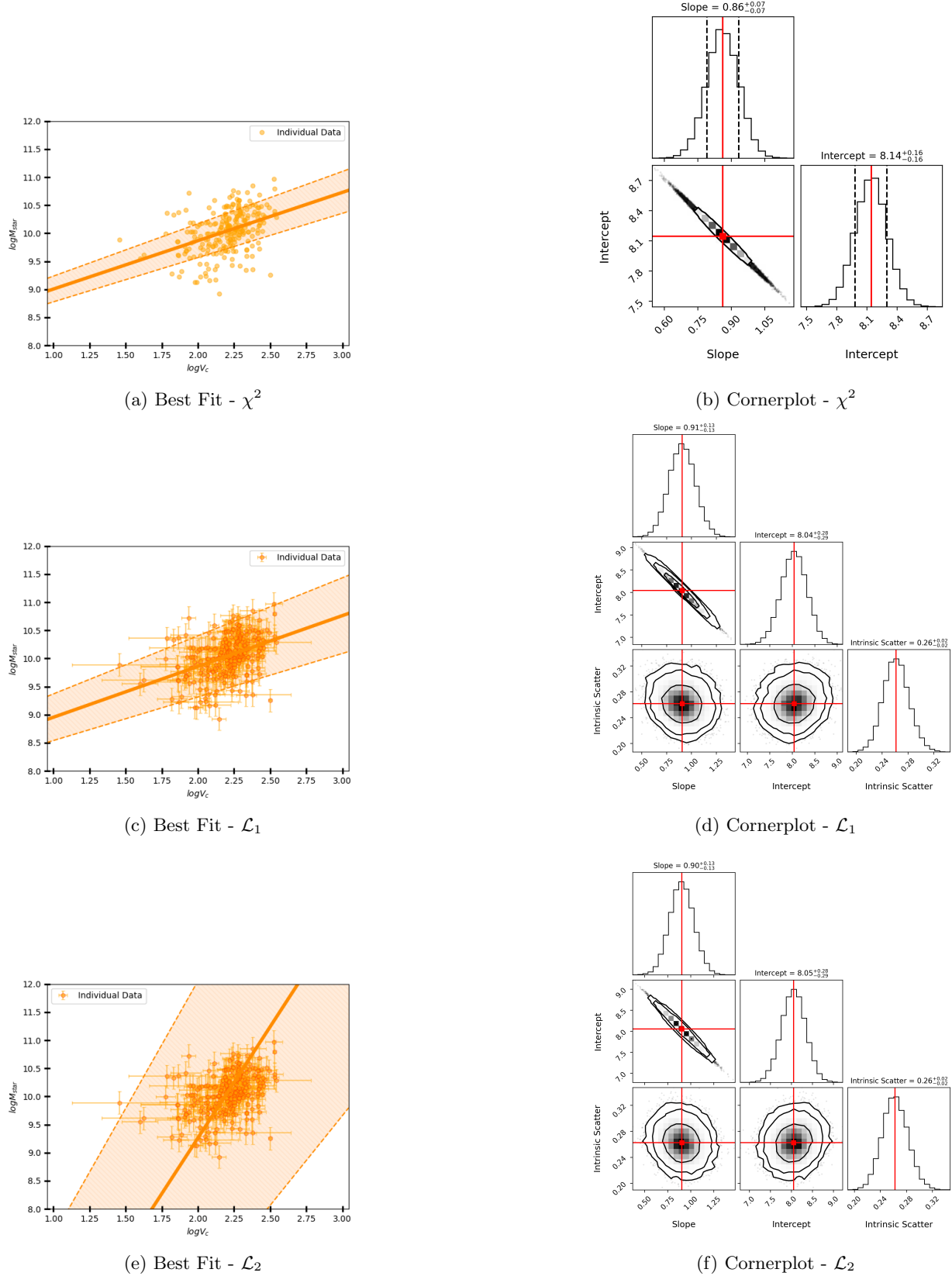


Figure 1.5: STFR - The posterior distribution and best-fit plots for the full masses using the three likelihoods.

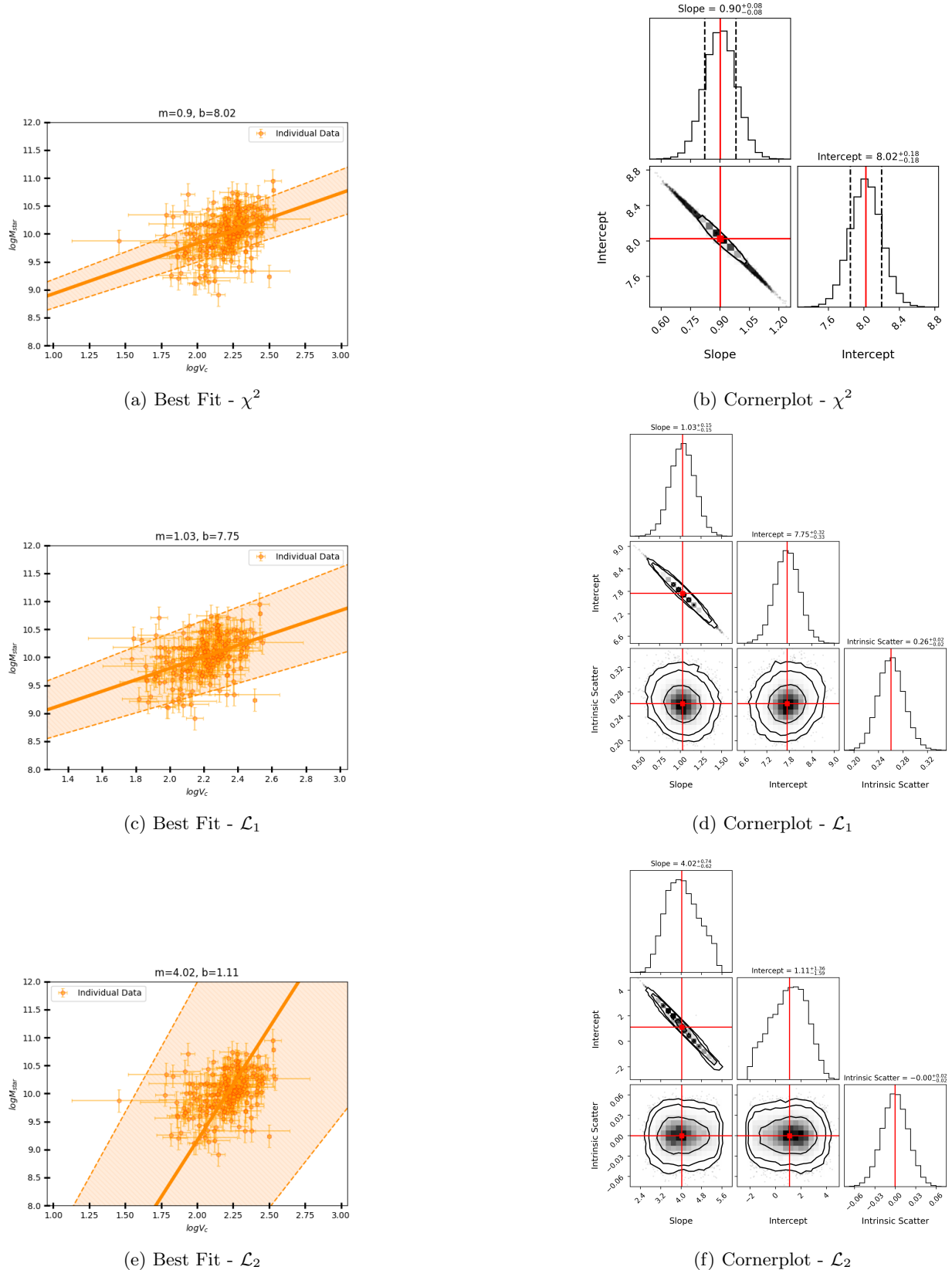


Figure 1.6: STFR – The posterior distribution and best-fit plots for the scaled down masses using the three likelihoods.

1.5 Conclusions

For our two datasets we concluded the following things

1. The slope and intercept parameters we attained for $z \sim 0$ agree with the ones in [Lel+19], meaning that we successfully recreated the results they did. We find that V_f shows the steepest slope and the least intrinsic scatter, making it a better velocity definition than the other 5 we considered.
2. The slopes in $z \sim 1$ are very small for BTFR and $m \sim 1$ for STFR. This implies little-to-no correlation which could be due to the high errors in our data or due to the computations done to arrive at the values for the masses and velocities. This does not however, stand as the final conclusion to the project as we are still working on doing the analysis on bigger datasets at the same redshift.

All the codes and figures used in this report can be found at <https://github.com/varenya27/Tully-Fisher>

Chapter 2

Linearity and Universality of Dark Matter in Galaxy Clusters

2.1 Abstract

We perform tests to search for the linearity and universality of dark matter in galaxy clusters. We use mass relations from [Che+07; Chi+18; CL22] to analyse the mass profiles and the dark to baryonic mass ratio $\frac{M_{dark}}{M_{bar}}$ up to r_{500} . We find that there is no preferred scale where the effect of dark matter kicks in, ie. dark matter is universal in galaxy clusters. We perform a linear fit on the ratio in hand against the radius and do a simple χ^2 test and compute p-values to see the validity of the fit. We see that most of the clusters show high χ^2 (and correspondingly, low p-values) implying that the ratio doesn't follow a linear relation. The clusters that apparently show low χ^2 values usually have considerably high errors in the parameters used to compute the masses.

2.2 Introduction

The dark matter problem is one of the most vexing problems in Modern Physics and Astrophysics. Although dark matter constitutes about 25% of total energy density of the universe and is a basic tenet of the Λ CDM model [Agh+20], its identity is still a mystery, despite close to 100 years of evidence [BH18]. There is also no laboratory evidence for some of the most well motivated dark matter candidates such as WIMP or the axion or through indirect searches which have only reported null results [Mer17; Gas16; Des+04; BD18]. Furthermore, the currently established Λ CDM model has also faced some tensions at scales smaller than 1 Mpc, such as such as the core/cusp problem, missing satellite problem, too big to fail problem, satellites plane problem etc [BB17; Wei+15]. Data on galactic scales have also revealed some scaling relations or correlations for spiral galaxies such as Radial Acceleration Relation [MLS16], Mass Acceleration discrepancy relation [FM12b], constancy of dark matter halo surface density [Don+09]. Therefore a large number of alternatives to the standard Λ CDM model have emerged such as Self-Interacting Dark Matter [Adh+22], Superfluid dark matter [BFK18], Warm Dark Matter [CAV00], Wave (or Fuzzy) Dark Matter [Fer21], Flavor Mixed Dark Matter [Med14], modified gravity which obviates the need for dark matter [FM12b; BZ22].

In order to ascertain if these small scales issues need a paradigm shift from Λ CDM or whether they can be explained using feedback processes from baryons, one should test the aforementioned relations with different astrophysical systems which possess dark matter. We know that Radial Acceleration relation does not hold for dwarf disk spirals, low surface brightness galaxies, elliptical galaxies and galaxy groups [DSF19; CDD22; GD21]

Another class of objects to test if the above correlations are universal are galaxy clusters. Galaxy clusters are the most massive virialized objects in the universe [AEM11; KB12; Vik+14], which have proved to be wonderful laboratories for galaxy evolution, Cosmology and Fundamental Physics [AEM11; Vik+14; Des18; BD21b; BD21a; Bor+22]. Galaxy clusters were the first astrophysical source which gave evidence for dark matter [Zwi33]. They have been shown to rule out the universality of Radial Acceleration Relation [Pra+21; Tia+20; CD20; PD21; Eck+22; CL22] and constancy of halo surface density [Cha14; GD20; GD21]. Therefore, they continue to be very good laboratories for testing some of the anomalies and deterministic scaling

relations obtained using spiral galaxies.

Most recently, Lovas (L22, hereafter) [Lov22] has found another intriguing property of dark matter haloes on galactic scales. Using 175 galaxies from the SPARC sample, L22 showed that the ratio of dark matter to baryonic matter ($\frac{M_{dark}(r)}{M_{bar}(r)}$) shows a linear scaling as a function of radius. The residuals from the linear relation are small with $\sigma=0.31$. When the radius is scaled using the radius (r_1) at which the aforementioned ratio is unity ($r_{norm} = mr$) where $m = 1/r_1$, they find that $r_{norm} = r$. This linear trend was seen for galaxies of diverse morphologies in the SPARC sample from pressure supported to rotationally supported galaxies. This linear scaling extends up to the last available kinematic data point [Lov22]. It is not immediately obvious whether the linear trend for the ratio of dark matter to baryonic matter can be reproduced from the current theory of structure formation involving the Λ CDM model. In order to test whether this linear trend as a function of radius is universal property of all dark matter haloes, we test this *ansatz* with galaxy clusters using the HIFLUGCS sample [Che+07].

2.3 Data and Analysis

The HIFLUGS cluster sample consists of 106 galaxy clusters and groups based on ROSAT and ASCA observations [Che+07; RB02]. Among these, 92 clusters have temperatures determined using X-ray spectroscopy whereas the remaining clusters had temperatures estimated using $L_x - T$ correlations [Mar98]. The X-ray surface brightness profiles have been obtained for 36 clusters from the RASS survey and from pointed ROSAT observations for the remaining 70. The imaging has been done up to a radius of r_{500} . This final sample consists of about 52 cool core clusters and 54 non-cool core clusters. More details on the observations and data reductions can be found in Refs. [Che+07; RB02].

The X-ray surface brightness profile was fit to both a single- β . The number density for a single- β profile was given by [CF76]

$$n(r) = n_0 \left(1 + \frac{r^2}{r_c^2}\right)^{-3\beta/2}, \quad (2.1)$$

where n_0 is the central density, r_c the core radius and β is the index parameter. Assuming that the cluster gas is in hydrostatic equilibrium, the total cluster mass is given by [Che+07]

$$M_{tot}(r) = \frac{3\beta T_h r}{G \mu m_p} \frac{(r/r_c)^2}{1 + (r/r_c)^2}, \quad (2.2)$$

where μ is the mean molecular weight equal to 0.59 [Che+07]. Eq. 2.2 assumes that the gas is a constant temperature T_h . This assumption is true for non-cool core clusters [Rei+13], where the temperature gradient in hot gas is less than 8% [Hud+10]. However, the isothermality will not be applicable to the central regions in cool core clusters. Therefore, our analysis, we only choose non-cool core clusters. All clusters with cooling time less than Hubble time (13 Gyr) are identified as cool-core clusters and not used for this work.

For the HIFLUGCS sample, 49 clusters show lower χ^2 with a double- β model fit to the gas density profile. However, no automated model selection techniques (such as AIC, BIC or Bayes factors) have been used to quantify the significance of goodness of fit of the double- β profile with respect to single- β model. Nevertheless, for this work we restrict our analysis to clusters for which single- β profile provides the minimum χ^2 . The best-fit values of all the parameters needed to estimate the hydrostatic mass from Eq. 2.2 are provided in Table 1 of [Che+07]. Our final sample used for this work consists of 54 non-cool core clusters.

To test the linearity we need the total dark matter in addition to the total mass distribution, which we know from Eq. 2.2:

$$M_{DM} = M_{tot}(r) - M_{gas}(r) - M_{stars}(r), \quad (2.3)$$

where M_{gas} is the total gas mass and M_{stars} is the total mass due to stars. The gas mass can be obtained by assuming spherical symmetry

$$M_{gas}(r) = m_g \int 4\pi r^2 n(r') dr', \quad (2.4)$$

where $n(r)$ is the gas density given in Eq. 2.1, m_g is the average mass of each gas particle and is given by μm_p . Although analytical expression for the integral in Eq. 2.4 have been provided [CL22], here we evaluate the integrals numerically to get the gas density at a given radius (r). To obtain M_{stars} , we used the stellar to gas mass relation from [Chi+18]. This relation was derived using a sample of 91 SPT-SZ clusters detected upto a range of 1.3.

We carried out our analysis till r_{500} (the radius enclosing 500 galaxies), and plotted the ratio $\frac{M_{dark}}{M_{bar}}$ as, seen in 2.1. We then ran a simple regression analysis using `scipy.optimize.curve_fit` (initializing the intercept to zero, which is expected in relations like these) to get a sense of the best fit "line" for our data. Using the parameters from the fit, we computed the χ^2 values for 10 evenly spaced points (following the general formula):

$$\chi^2 = \sum \left(\frac{y_i - (mx_i + b)}{\sigma_y} \right)^2, \quad (2.5)$$

The χ^2 values for each cluster tell us about how "good" the fit is. A high χ^2 usually means that the fit is bad. We also calculated p-values of the models from the χ^2 analysis and set the usual threshold of 0.05, below which the null hypothesis cannot be rejected (ie. the data does not fit the model). The p-value is calculated for the 9 degrees of freedom (since we have 10 sampled points and one parameter- the slope).

2.4 Results

The results for the χ^2 and p-value are presented in Table 2.1

Cluster Name	χ^2	p-value	Cluster Name	χ^2	p-value
A0119	205.74	0.00	MKW8	16.53	0.09
A0399	14.98	0.13	ZwCl 1215	9.68	0.47
A0400	231.32	0.00	3C 129	7.10	0.72
A0401	476.93	0.00	A0548e	215.64	0.00
A0576	3.56	0.96	A0548w	5.12	0.88
A0754	262.93	0.00	A1775	108.85	0.00
A1367	201.06	0.00	A1800	3.34	0.97
A1644	12.20	0.27	A2319	440.38	0.00
A1650	15.27	0.12	A2734	105.08	0.00
A1736	7.52	0.68	A2877	10.07	0.43
A2065	1.61	1.00	A3395n	2.19	0.99
A2147	25.57	0.00	A3528n	104.52	0.00
A2163	98.53	0.00	A3530	25.53	0.00
A2255	106.40	0.00	A3532	109.87	0.00
A2256	100.95	0.00	A3560	13.05	0.22
A2634	67.82	0.00	A3627	65.63	0.00
A3158	221.25	0.00	A3695	3.75	0.96
A3266	312.30	0.00	A3822	9.84	0.45
A3376	29.33	0.00	A3827	2.65	0.99
A3391	122.26	0.00	A3888	6.94	0.73
A3395s	7.00	0.72	A3921	117.15	0.00
A3558	1112.25	0.00	IIZw 108	5.37	0.87
A3562	500.08	0.00	OPHIUCHU	181.25	0.00
A3667	577.97	0.00	RXJ2344	9.16	0.52
COMA	157.47	0.00	S405	3.45	0.97
FORNAX	33.12	0.00	S636	7.87	0.64
IIZw54	3.65	0.96	TRIANGUL	764.66	0.00

Table 2.1: The χ^2 values are clearly very high for most of the clusters. The clusters with relatively low χ^2 values usually have very large errors (> 0.5) in the quantities used to calculate them.

It is clear from this data that a linear fit, isn't accurate for the ratio of dark to baryonic matter in galaxy clusters. Fig 2.1 depicts the fits against the data along with the mass profiles of 4 selected clusters out of the 54 analysed ones.

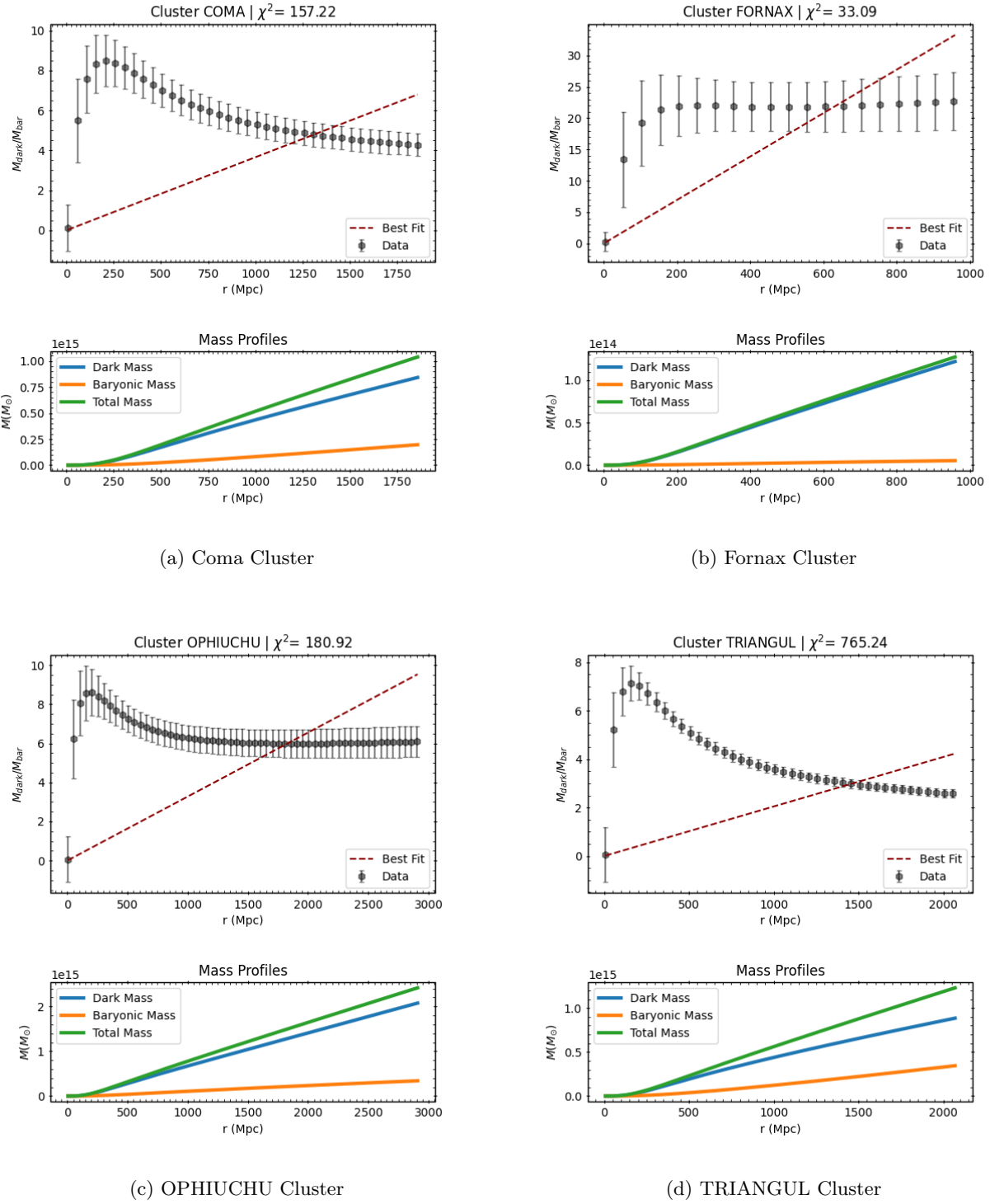


Figure 2.1: Dark to Baryonic Mass Ratio and Mass Profiles

It is also important to see the plots for the clusters with low χ^2 values, which supposedly point towards a linear model for our data. Fig 2.2 shows that a linear model, albeit suggested, looks absurd.

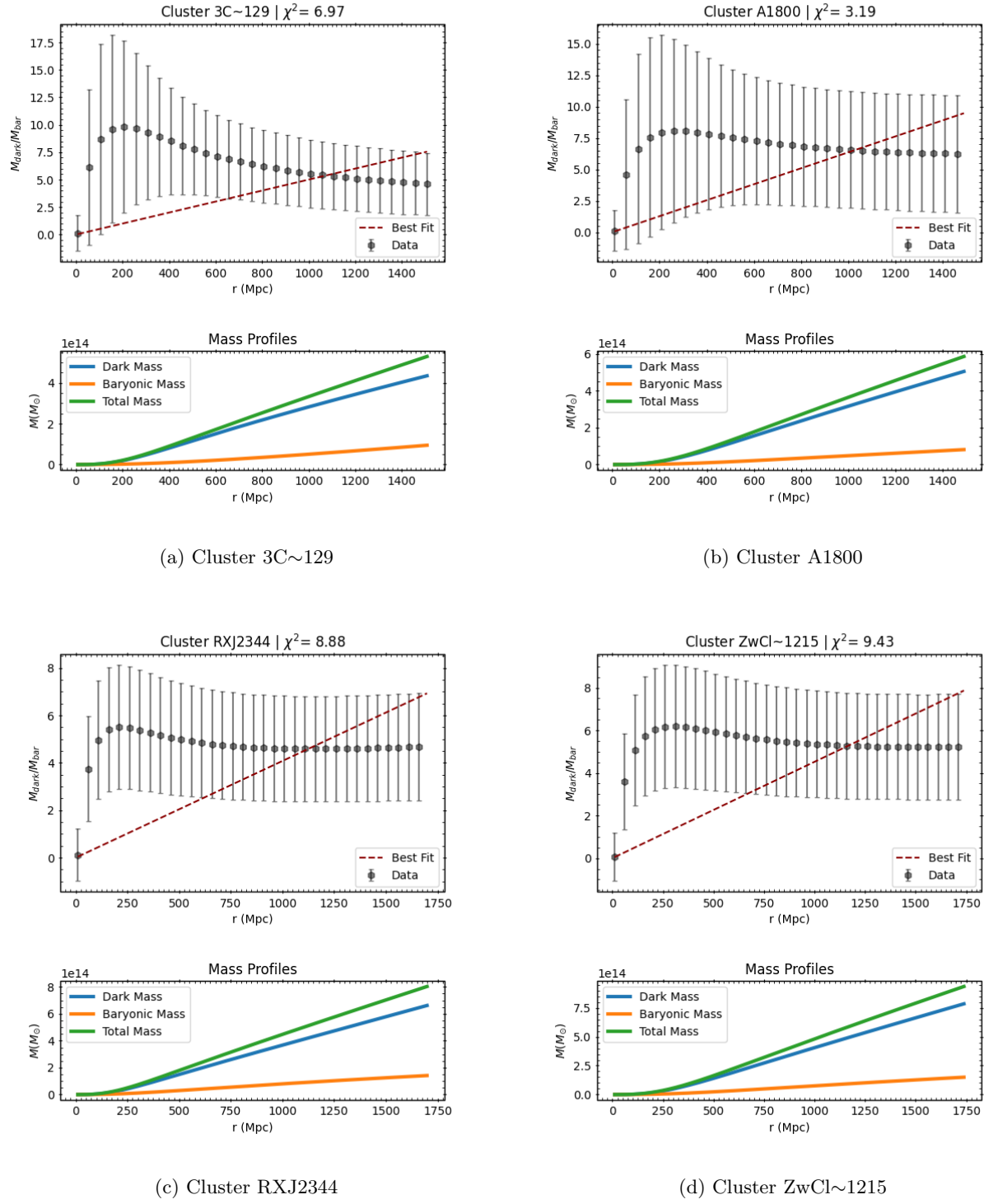


Figure 2.2: Dark to Baryonic Mass Ratio and Mass Profiles for clusters with high errors

2.5 Conclusion

We find that there is no preferred scale where the effect of dark matter kicks in (from the mass profiles), ie. dark matter is universal in galaxy clusters. The linear fitting of the data shows us that most of the clusters show high χ^2 (and correspondingly, low p-values) implying that the ratio doesn't follow a linear relation. The

clusters that apparently show low χ^2 values usually have considerably high errors in the parameters used to compute the masses.

All the codes and figures used in this report can be found at <https://github.com/varenya27/Galaxy-Clusters>

Bibliography

- [Zwi33] F. Zwicky. “Die Rotverschiebung von extragalaktischen Nebeln”. In: *Helvetica Physica Acta* 6 (Jan. 1933), pp. 110–127.
- [Ser63] J. L. Sersic. “Influence of the atmospheric and instrumental dispersion on the brightness distribution in a galaxy”. In: *Boletin de la Asociacion Argentina de Astronomia La Plata Argentina* 6 (Feb. 1963), pp. 41–43.
- [CF76] A. Cavaliere and R. Fusco-Femiano. “X-rays from hot plasma in clusters of galaxies.” In: *Astron. & Astrophys.* 49 (May 1976), pp. 137–144.
- [TF77] R. B. Tully and J. R. Fisher. “A new method of determining distances to galaxies.” In: *Astron. & Astrophys.* 54 (Feb. 1977), pp. 661–673.
- [Cou97] Stephane Courteau. “Optical Rotation Curves and Linewidths for Tully-Fisher Applications”. In: *The Astronomical Journal* 114 (Dec. 1997), p. 2402. DOI: [10.1086/118656](https://doi.org/10.1086/118656). URL: <https://doi.org/10.1086/118656>.
- [Mar98] Maxim Markevitch. “The L_X -T Relation and Temperature Function for Nearby Clusters Revisited”. In: *Astrophys. J.* 504.1 (Sept. 1998), pp. 27–34. DOI: [10.1086/306080](https://doi.org/10.1086/306080). arXiv: [astro-ph/9802059 \[astro-ph\]](https://arxiv.org/abs/astro-ph/9802059).
- [SN99] Matthias Steinmetz and Julio F. Navarro. “The Cosmological Origin of the Tully-Fisher Relation”. In: *The Astrophysical Journal* 513.2 (Mar. 1999), pp. 555–560. DOI: [10.1086/306904](https://doi.org/10.1086/306904). URL: <https://doi.org/10.1086/306904>.
- [CAV00] Pedro Colin, Vladimir Avila-Reese, and Octavio Valenzuela. “Substructure and Halo Density Profiles in a Warm Dark Matter Cosmology”. In: *Astrophys. J.* 542.2 (Oct. 2000), pp. 622–630. DOI: [10.1086/317057](https://doi.org/10.1086/317057). arXiv: [astro-ph/0004115 \[astro-ph\]](https://arxiv.org/abs/astro-ph/0004115).
- [KSW00] Jin Koda, Yoshiaki Sofue, and Keiichi Wada. “On the Origin of the Tully-Fisher Relation”. In: *The Astrophysical Journal* 532.1 (Mar. 2000), pp. 214–220. DOI: [10.1086/308579](https://doi.org/10.1086/308579). URL: <https://doi.org/10.1086/308579>.
- [McG+00] S. S. McGaugh et al. “The Baryonic Tully-Fisher Relation”. In: *The Astrophysical Journal* 533.2 (Apr. 2000), pp. L99–L102. DOI: [10.1086/312628](https://doi.org/10.1086/312628). URL: <https://doi.org/10.1086/312628>.
- [RB02] Thomas H. Reiprich and Hans Böhringer. “The Mass Function of an X-Ray Flux-limited Sample of Galaxy Clusters”. In: *Astrophys. J.* 567.2 (Mar. 2002), pp. 716–740. DOI: [10.1086/338753](https://doi.org/10.1086/338753). arXiv: [astro-ph/0111285 \[astro-ph\]](https://arxiv.org/abs/astro-ph/0111285).
- [Bel+03] Eric F. Bell et al. “A First Estimate of the Baryonic Mass Function of Galaxies”. In: *The Astrophysical Journal* 585.2 (Mar. 2003), pp. L117–L120. DOI: [10.1086/374389](https://doi.org/10.1086/374389). URL: <https://doi.org/10.1086/374389>.
- [Des+04] S. Desai et al. “Search for dark matter WIMPs using upward through-going muons in Super-Kamiokande”. In: *Phys. Rev. D* 70 (2004), p. 083523. DOI: [10.1103/PhysRevD.70.083523](https://doi.org/10.1103/PhysRevD.70.083523). arXiv: [hep-ex/0404025](https://arxiv.org/abs/hep-ex/0404025).
- [Che+07] Y. Chen et al. “Statistics of X-ray observables for the cooling-core and non-cooling core galaxy clusters”. In: *Astron. & Astrophys.* 466.3 (May 2007), pp. 805–812. DOI: [10.1051/0004-6361:20066471](https://doi.org/10.1051/0004-6361:20066471). arXiv: [astro-ph/0702482 \[astro-ph\]](https://arxiv.org/abs/astro-ph/0702482).
- [Cou+09] Helene M. Courtois et al. “The Extragalactic Distance Database: All Digital H I Profile Catalog”. In: *Astron. J.* 138.6 (Dec. 2009), pp. 1938–1956. DOI: [10.1088/0004-6256/138/6/1938](https://doi.org/10.1088/0004-6256/138/6/1938). arXiv: [0902.3670 \[astro-ph.CO\]](https://arxiv.org/abs/0902.3670).

- [Don+09] F. Donato et al. “A constant dark matter halo surface density in galaxies”. In: *Mon. Not. R. Astron. Soc.* 397.3 (Aug. 2009), pp. 1169–1176. DOI: [10.1111/j.1365-2966.2009.15004.x](https://doi.org/10.1111/j.1365-2966.2009.15004.x). arXiv: [0904.4054 \[astro-ph.CO\]](https://arxiv.org/abs/0904.4054).
- [Tra+09] C. Trachternach et al. “The baryonic Tully-Fisher relation and its implication for dark matter halos”. In: *Astronomy & Astrophysics* 505.2 (Aug. 2009), pp. 577–587. DOI: [10.1051/0004-6361/200811136](https://doi.org/10.1051/0004-6361/200811136). URL: <https://doi.org/10.1051%2F0004-6361%2F200811136>.
- [Hud+10] D. S. Hudson et al. “What is a cool-core cluster? a detailed analysis of the cores of the X-ray flux-limited HIFLUGCS cluster sample”. In: *Astron. & Astrophys.* 513, A37 (Apr. 2010), A37. DOI: [10.1051/0004-6361/200912377](https://doi.org/10.1051/0004-6361/200912377). arXiv: [0911.0409 \[astro-ph.CO\]](https://arxiv.org/abs/0911.0409).
- [AEM11] Steven W. Allen, August E. Evrard, and Adam B. Mantz. “Cosmological Parameters from Observations of Galaxy Clusters”. In: *Ann. Rev. Astron. Astrophys.* 49.1 (Sept. 2011), pp. 409–470. DOI: [10.1146/annurev-astro-081710-102514](https://doi.org/10.1146/annurev-astro-081710-102514). arXiv: [1103.4829 \[astro-ph.CO\]](https://arxiv.org/abs/1103.4829).
- [FM12a] Benoit Famaey and Stacy S. McGaugh. “Modified Newtonian Dynamics (MOND): Observational Phenomenology and Relativistic Extensions”. In: *Living Reviews in Relativity* 15.1, 10 (Sept. 2012), p. 10. DOI: [10.12942/lrr-2012-10](https://doi.org/10.12942/lrr-2012-10). arXiv: [1112.3960 \[astro-ph.CO\]](https://arxiv.org/abs/1112.3960).
- [FM12b] Benoit Famaey and Stacy S. McGaugh. “Modified Newtonian Dynamics (MOND): Observational Phenomenology and Relativistic Extensions”. In: *Living Reviews in Relativity* 15.1, 10 (Sept. 2012), p. 10. DOI: [10.12942/lrr-2012-10](https://doi.org/10.12942/lrr-2012-10). arXiv: [1112.3960 \[astro-ph.CO\]](https://arxiv.org/abs/1112.3960).
- [KB12] Andrey V. Kravtsov and Stefano Borgani. “Formation of Galaxy Clusters”. In: *Ann. Rev. Astron. Astrophys.* 50 (Sept. 2012), pp. 353–409. DOI: [10.1146/annurev-astro-081811-125502](https://doi.org/10.1146/annurev-astro-081811-125502). arXiv: [1205.5556 \[astro-ph.CO\]](https://arxiv.org/abs/1205.5556).
- [For+13] Daniel Foreman-Mackey et al. “emcee: The MCMC Hammer”. In: *Publications of the Astronomical Society of the Pacific* 125.925 (Mar. 2013), pp. 306–312. DOI: [10.1086/670067](https://doi.org/10.1086/670067). URL: <https://doi.org/10.1086%2F670067>.
- [Rei+13] Thomas H. Reiprich et al. “Outskirts of Galaxy Clusters”. In: *Space Science Revs.* 177.1-4 (Aug. 2013), pp. 195–245. DOI: [10.1007/s11214-013-9983-8](https://doi.org/10.1007/s11214-013-9983-8). arXiv: [1303.3286 \[astro-ph.CO\]](https://arxiv.org/abs/1303.3286).
- [Cha14] M. H. Chan. “A tight scaling relation of dark matter in galaxy clusters.” In: *Mon. Not. R. Astron. Soc.* 442 (July 2014), pp. L14–L17. DOI: [10.1093/mnrasl/slu047](https://doi.org/10.1093/mnrasl/slu047). arXiv: [1403.4352 \[astro-ph.CO\]](https://arxiv.org/abs/1403.4352).
- [Med14] Mikhail V. Medvedev. “Cosmological Simulations of Multicomponent Cold Dark Matter”. In: *Physical Review Letters* 113.7, 071303 (Aug. 2014), p. 071303. DOI: [10.1103/PhysRevLett.113.071303](https://doi.org/10.1103/PhysRevLett.113.071303). arXiv: [1305.1307 \[astro-ph.CO\]](https://arxiv.org/abs/1305.1307).
- [Vik+14] A. A. Vikhlinin et al. “Clusters of galaxies”. In: *Physics Uspekhi* 57, 317-341 (Apr. 2014), pp. 317–341. DOI: [10.3367/UFNe.0184.201404a.0339](https://doi.org/10.3367/UFNe.0184.201404a.0339).
- [Wei+15] David H. Weinberg et al. “Cold dark matter: Controversies on small scales”. In: *Proceedings of the National Academy of Science* 112.40 (Oct. 2015), pp. 12249–12255. DOI: [10.1073/pnas.1308716112](https://doi.org/10.1073/pnas.1308716112). arXiv: [1306.0913 \[astro-ph.CO\]](https://arxiv.org/abs/1306.0913).
- [Gas16] Jennifer M. Gaskins. “A review of indirect searches for particle dark matter”. In: *Contemporary Physics* 57.4 (Oct. 2016), pp. 496–525. DOI: [10.1080/00107514.2016.1175160](https://doi.org/10.1080/00107514.2016.1175160). arXiv: [1604.00014 \[astro-ph.HE\]](https://arxiv.org/abs/1604.00014).
- [LMS16] Federico Lelli, Stacy S. McGaugh, and James M. Schombert. “SPARC: Mass Models for 175 Disk Galaxies with Spitzer Photometry and Accurate Rotation Curves”. In: *Astron. J.* 152.6, 157 (Dec. 2016), p. 157. DOI: [10.3847/0004-6256/152/6/157](https://doi.org/10.3847/0004-6256/152/6/157). arXiv: [1606.09251 \[astro-ph.GA\]](https://arxiv.org/abs/1606.09251).
- [MLS16] Stacy S. McGaugh, Federico Lelli, and James M. Schombert. “Radial Acceleration Relation in Rotationally Supported Galaxies”. In: *Physical Review Letters* 117.20, 201101 (Nov. 2016), p. 201101. DOI: [10.1103/PhysRevLett.117.201101](https://doi.org/10.1103/PhysRevLett.117.201101). arXiv: [1609.05917 \[astro-ph.GA\]](https://arxiv.org/abs/1609.05917).
- [Sto+16] John P. Stott et al. “The KMOS Redshift One Spectroscopic Survey (KROSS): dynamical properties, gas and dark matter fractions of typical $z \sim 1$ star-forming galaxies”. In: *Monthly Notices of the Royal Astronomical Society* 457.2 (Feb. 2016), pp. 1888–1904. DOI: [10.1093/mnras/stw129](https://doi.org/10.1093/mnras/stw129). URL: <https://doi.org/10.1093%2Fmnras%2Fstw129>.

- [BB17] James S. Bullock and Michael Boylan-Kolchin. “Small-Scale Challenges to the Λ CDM Paradigm”. In: *Ann. Rev. Astron. Astrophys.* 55.1 (Aug. 2017), pp. 343–387. DOI: [10.1146/annurev-astro-091916-055313](https://doi.org/10.1146/annurev-astro-091916-055313). arXiv: [1707.04256 \[astro-ph.CO\]](https://arxiv.org/abs/1707.04256).
- [Mer17] David Merritt. “Cosmology and convention”. In: *Studies in the History and Philosophy of Modern Physics* 57 (Feb. 2017), pp. 41–52. DOI: [10.1016/j.shpsb.2016.12.002](https://doi.org/10.1016/j.shpsb.2016.12.002). arXiv: [1703.02389 \[physics.hist-ph\]](https://arxiv.org/abs/1703.02389).
- [BFK18] Lasha Berezhiani, Benoit Famaey, and Justin Khoury. “Phenomenological consequences of superfluid dark matter with baryon-phonon coupling”. In: *JCAP* 2018.9, 021 (Sept. 2018), p. 021. DOI: [10.1088/1475-7516/2018/09/021](https://doi.org/10.1088/1475-7516/2018/09/021). arXiv: [1711.05748 \[astro-ph.CO\]](https://arxiv.org/abs/1711.05748).
- [BH18] Gianfranco Bertone and Dan Hooper. “History of dark matter”. In: *Reviews of Modern Physics* 90.4, 045002 (Oct. 2018), p. 045002. DOI: [10.1103/RevModPhys.90.045002](https://doi.org/10.1103/RevModPhys.90.045002). arXiv: [1605.04909 \[astro-ph.CO\]](https://arxiv.org/abs/1605.04909).
- [BD18] Antonio Boveia and Caterina Doglioni. “Dark Matter Searches at Colliders”. In: *Annual Review of Nuclear and Particle Science* 68 (Oct. 2018), pp. 429–459. DOI: [10.1146/annurev-nucl-101917-021008](https://doi.org/10.1146/annurev-nucl-101917-021008). arXiv: [1810.12238 \[hep-ex\]](https://arxiv.org/abs/1810.12238).
- [Chi+18] I. Chiu et al. “Baryon content in a sample of 91 galaxy clusters selected by the South Pole Telescope at $0.2 \leq z \leq 1.25$ ”. In: *Mon. Not. R. Astron. Soc.* 478.3 (Aug. 2018), pp. 3072–3099. DOI: [10.1093/mnras/sty1284](https://doi.org/10.1093/mnras/sty1284). arXiv: [1711.00917 \[astro-ph.CO\]](https://arxiv.org/abs/1711.00917).
- [Des18] S. Desai. “Limit on graviton mass from galaxy cluster Abell 1689”. In: *Physics Letters B* 778 (Feb. 2018), pp. 325–331. DOI: [10.1016/j.physletb.2018.01.052](https://doi.org/10.1016/j.physletb.2018.01.052). arXiv: [1708.06502](https://arxiv.org/abs/1708.06502).
- [HF18] David W. Hogg and Daniel Foreman-Mackey. “Data Analysis Recipes: Using Markov Chain Monte Carlo”. In: *The Astrophysical Journal Supplement Series* 236.1 (May 2018), p. 11. DOI: [10.3847/1538-4365/aab76e](https://doi.org/10.3847/1538-4365/aab76e). URL: <https://doi.org/10.3847%2F1538-4365%2Faab76e>.
- [DSF19] C. Di Paolo, P. Salucci, and J. P. Fontaine. “The Radial Acceleration Relation (RAR): Crucial Cases of Dwarf Disks and Low-surface-brightness Galaxies”. In: *Astrophys. J.* 873.2, 106 (Mar. 2019), p. 106. DOI: [10.3847/1538-4357/aaffd6](https://doi.org/10.3847/1538-4357/aaffd6). arXiv: [1810.08472 \[astro-ph.GA\]](https://arxiv.org/abs/1810.08472).
- [Lel+19] Federico Lelli et al. “The baryonic Tully-Fisher relation for different velocity definitions and implications for galaxy angular momentum”. In: *Mon. Not. R. Astron. Soc.* 484.3 (Apr. 2019), pp. 3267–3278. DOI: [10.1093/mnras/stz205](https://doi.org/10.1093/mnras/stz205). arXiv: [1901.05966 \[astro-ph.GA\]](https://arxiv.org/abs/1901.05966).
- [Agh+20] N. Aghanim et al. “Planck 2018 results. VI. Cosmological parameters”. In: *Astron. Astrophys.* 641 (2020). [Erratum: *Astron. Astrophys.* 652, C4 (2021)], A6. DOI: [10.1051/0004-6361/201833910](https://doi.org/10.1051/0004-6361/201833910). arXiv: [1807.06209 \[astro-ph.CO\]](https://arxiv.org/abs/1807.06209).
- [CD20] Man Ho Chan and Antonino Del Popolo. “The radial acceleration relation in galaxy clusters”. In: *Mon. Not. R. Astron. Soc.* (Jan. 2020), p. 218. DOI: [10.1093/mnras/staa225](https://doi.org/10.1093/mnras/staa225). arXiv: [2001.06141 \[astro-ph.GA\]](https://arxiv.org/abs/2001.06141).
- [GD20] K. Gopika and Shantanu Desai. “Scaling relations for dark matter core density and radius from Chandra X-ray cluster sample”. In: *Physics of the Dark Universe* 30, 100707 (Dec. 2020), p. 100707. DOI: [10.1016/j.dark.2020.100707](https://doi.org/10.1016/j.dark.2020.100707). arXiv: [2006.12320 \[astro-ph.CO\]](https://arxiv.org/abs/2006.12320).
- [Tia+20] Yong Tian et al. “The Radial Acceleration Relation in CLASH Galaxy Clusters”. In: *Astrophys. J.* 896.1, 70 (June 2020), p. 70. DOI: [10.3847/1538-4357/ab8e3d](https://doi.org/10.3847/1538-4357/ab8e3d). arXiv: [2001.08340 \[astro-ph.CO\]](https://arxiv.org/abs/2001.08340).
- [BD21a] Kamal Bora and Shantanu Desai. “A test of cosmic distance duality relation using SPT-SZ galaxy clusters, Type Ia supernovae, and cosmic chronometers”. In: *JCAP* 2021.6, 052 (June 2021), p. 052. DOI: [10.1088/1475-7516/2021/06/052](https://doi.org/10.1088/1475-7516/2021/06/052). arXiv: [2104.00974 \[astro-ph.CO\]](https://arxiv.org/abs/2104.00974).
- [BD21b] Kamal Bora and Shantanu Desai. “Constraints on the variation of fine structure constant from joint SPT-SZ and XMM-Newton observations”. In: *JCAP* 2021.2, 012 (Feb. 2021), p. 012. DOI: [10.1088/1475-7516/2021/02/012](https://doi.org/10.1088/1475-7516/2021/02/012). arXiv: [2008.10541 \[astro-ph.CO\]](https://arxiv.org/abs/2008.10541).
- [Fer21] Elisa G. M. Ferreira. “Ultra-light dark matter”. In: *Astron and Astrophys Reviews* 29.1, 7 (Dec. 2021), p. 7. DOI: [10.1007/s00159-021-00135-6](https://doi.org/10.1007/s00159-021-00135-6). arXiv: [2005.03254 \[astro-ph.CO\]](https://arxiv.org/abs/2005.03254).

- [GD21] K. Gopika and Shantanu Desai. “A test of constancy of dark matter halo surface density and radial acceleration relation in relaxed galaxy groups”. In: *Physics of the Dark Universe* 33, 100874 (Sept. 2021), p. 100874. DOI: [10.1016/j.dark.2021.100874](https://doi.org/10.1016/j.dark.2021.100874). arXiv: [2106.07294](https://arxiv.org/abs/2106.07294) [[astro-ph.CO](#)].
- [PD21] S. Pradyumna and Shantanu Desai. “A test of Radial Acceleration Relation for the Giles et al Chandra cluster sample”. In: *Physics of the Dark Universe* 33, 100854 (Sept. 2021), p. 100854. DOI: [10.1016/j.dark.2021.100854](https://doi.org/10.1016/j.dark.2021.100854). arXiv: [2107.05845](https://arxiv.org/abs/2107.05845) [[astro-ph.CO](#)].
- [Pra+21] S. Pradyumna et al. “Yet another test of Radial Acceleration Relation for galaxy clusters”. In: *Physics of the Dark Universe* 31, 100765 (Jan. 2021), p. 100765. DOI: [10.1016/j.dark.2020.100765](https://doi.org/10.1016/j.dark.2020.100765). arXiv: [2011.06421](https://arxiv.org/abs/2011.06421) [[astro-ph.CO](#)].
- [Sha+21] Gauri Sharma et al. “Flat rotation curves of $z \sim 1$ star-forming galaxies”. In: *Mon. Not. R. Astron. Soc.* 503.2 (May 2021), pp. 1753–1772. DOI: [10.1093/mnras/stab249](https://doi.org/10.1093/mnras/stab249). arXiv: [2005.00279](https://arxiv.org/abs/2005.00279) [[astro-ph.GA](#)].
- [Adh+22] Susmita Adhikari et al. “Astrophysical Tests of Dark Matter Self-Interactions”. In: *arXiv e-prints*, arXiv:2207.10638 (July 2022), arXiv:2207.10638. arXiv: [2207.10638](https://arxiv.org/abs/2207.10638) [[astro-ph.CO](#)].
- [BZ22] Indranil Banik and Hongsheng Zhao. “From Galactic Bars to the Hubble Tension: Weighing Up the Astrophysical Evidence for Milgromian Gravity”. In: *Symmetry* 14.7 (June 2022), p. 1331. DOI: [10.3390/sym14071331](https://doi.org/10.3390/sym14071331). arXiv: [2110.06936](https://arxiv.org/abs/2110.06936) [[astro-ph.CO](#)].
- [Bor+22] Kamal Bora et al. “A test of the standard dark matter density evolution law using galaxy clusters and cosmic chronometers”. In: *European Physical Journal C* 82.1, 17 (Jan. 2022), p. 17. DOI: [10.1140/epjc/s10052-022-09987-3](https://doi.org/10.1140/epjc/s10052-022-09987-3). arXiv: [2106.15805](https://arxiv.org/abs/2106.15805) [[astro-ph.CO](#)].
- [CDD22] Man Ho Chan, Shantanu Desai, and Antonino Del Popolo. “There is no universal acceleration scale in galaxies”. In: *arXiv e-prints*, arXiv:2205.07515 (May 2022), arXiv:2205.07515. arXiv: [2205.07515](https://arxiv.org/abs/2205.07515) [[astro-ph.GA](#)].
- [CL22] Man Ho Chan and Ka Chung Law. “Analytic radial acceleration relation for galaxy clusters”. In: *Physical Review D* 105.8, 083003 (Apr. 2022), p. 083003. DOI: [10.1103/PhysRevD.105.083003](https://doi.org/10.1103/PhysRevD.105.083003). arXiv: [2203.15217](https://arxiv.org/abs/2203.15217) [[astro-ph.CO](#)].
- [Eck+22] D. Eckert et al. “The gravitational field of X-COP galaxy clusters”. In: *Astron. & Astrophys.* 662, A123 (June 2022), A123. DOI: [10.1051/0004-6361/202142507](https://doi.org/10.1051/0004-6361/202142507). arXiv: [2205.01110](https://arxiv.org/abs/2205.01110) [[astro-ph.CO](#)].
- [Lov22] Stephen Lovas. “Linearity: galaxy formation encounters an unanticipated empirical relation”. In: *Mon. Not. R. Astron. Soc.* 514.1 (July 2022), pp. L56–L60. DOI: [10.1093/mnrasl/slac056](https://doi.org/10.1093/mnrasl/slac056). arXiv: [2206.11431](https://arxiv.org/abs/2206.11431) [[astro-ph.GA](#)].